Aalborg Universitet

AALBORG UNIVERSITY

DENMARK

Multilayer Control for Inverters in Parallel Operation without Intercommunications

Hua, Ming ; Hu, Haibing; Xing, Yan ; Guerrero, Josep M.

Multilayer Control for Inverters in Parallel Operation

without Signal Interconnection

Ming Hua[1], *Student Member, IEEE*, Haibing Hu[1], *Member, IEEE*, Yan Xing[1], *Member, IEEE*, and

Josep M. Guerrero[2], *Senior Member, IEEE*

1. Jiangsu Key Lab. of New Energy Generation and Power Conversion, NUAA, Nanjing 210016, P.R. China

2. Dept. Energy Technology, Aalborg University, DK-9220, Aalborg, Denmark

Corresponding author: Ming Hua, Tel: +86-25-84890393, Fax: +86-25-84890393, E-mail: huaming@nuaa.edu.cn

Abstract—**In this paper, a multilayer control is proposed for inverters able to operate in parallel without intercommunications. The first layer control is an improved droop method by introducing power proportional terms into a conventional droop scheme, which let both the active and reactive power to be shared among the modules. The second layer is designed to compensate the voltage droop caused by the droop control mentioned and improve the load regulation performance of the system. The third layer is a quasi-synchronization control aiming to adjust roughly and ensure the phase deviation among the inverters within a limited margin with the help of the phase signal sensed from the shared ac output power bus. The operational principle and implementation are analyzed with design consideration given in detail. Experimental results with a prototype system of two 35kVA inverters verify the analysis and design.**

Index Terms-- **Inverters, parallel operation, droop method, quasi-synchronization control, multilayer control**

I. INTRODUCTION

MORE and more DC and AC power supply systems requiring large capacity, high reliability, and standard structure are realized by operating multiple power modules in parallel. Many control methods for such a parallel inverter system have been proposed. In general, these control mentioned may be categorized as centralized control, distributed control and wireless control [1]-[2]. And among them the wireless control, which means there is no signal interconnection among the inverters in parallel, has been caught great attention due to its low dependency on communications, and its application in areas like Microgrids (MG) or distributed UPS systems. This control method is based on adjusting the frequency and amplitude references according to the inverter output active and reactive power [3]-[28], [30]. However, although the technique achieves high reliability and flexibility, it has several drawbacks that limit its performance.

First, conventional droop control may lead to instability since it introduces a positive feedback in certain conditions. In order to avoid this possible positive feedback, in [25], a control variation has been proposed, which decouples the frequency and voltage droops by taking into consideration the line impedance and load. However the decoupling control is complex since it relies on power line parameters and types of loads.

Besides, another important disadvantage of the conventional droop method is its load-dependent frequency and amplitude deviations which induce to poor performance in load regulation [26]. There is an inherent trade-off between the voltage regulation and the current sharing between the inverters [27]. Reference [28] proposes a strategy to improve the control technique by means of changing the droop coefficient and estimating the effect of the line impedance value. However, the strategy is quite complicated and sensitive to parameter tolerance. In [26], a controller has been proposed in order to restore the nominal values of the voltage by introducing an integrator inside the MG. However, in practical the mismatches among the parameters may cause larger circulating currents even instability. Hierarchical control applied to power dispatching in AC power systems is well known and it has been used extensively for decades [29]. UCTE (Union for the Co-ordination of Transmission of Electricity, Continental Europe) has been defined a hierarchical control for large power system, which is supposed to operate very high-power synchronous machines with high inertias and inductive networks [30]. Thanks to the hierarchical control, the amplitude and frequency deviations are limited and thus the system power quality, reliability and stability are improved. In [30], a general approach of hierarchical control is proposed with a secondary control introduced to bring the deviated voltage and frequency back to the rated values. However, a centralized controller and low bandwidth communication among the inverters have to be employed in the control.

Nevertheless, the transient response and the hot-swap performance are not so good under wireless control since there is no information exchanged among the parallel inverters. Referencing the achievement of parallel control with control interconnection,

pre-synchronizing the reference signals of inverters beyond the current sharing control helps greatly to improve the dynamic performance, especially during hot-swap [1]-[2], [31].

In this paper, buying the idea of hierarchical control, a multilayer wireless control for three phase inverters in parallel operation is proposed. The operational principle of the three control layers, an improved droop control, output voltage compensation and a reference-voltage pre-synchronization, and the coordination among them are analyzed in detail with the stability and design consideration given. Experimental results with a prototype system of two 35kVA inverters verify excellent dynamic performance, especially during hot plug-in, stability and reliability of the control proposed.

II. PRINCIPLE OF THE MULTILAYER CONTROL PROPOSED

The popular six-switch three-phase inverter topology is employed. The inverters are ended by LCL filters, being the inner L and C the harmonics filter, and the output inductor is the current-sharing-inductor, L_{pa}, connecting the output of the inverter to the common ac power bus. The conventional dual loop PI control and space vector modulation are employed to regulate the output voltage for each inverter. We know that the equivalent model of the inverter can be looked upon a DC system in dq rotation frame, and the equivalent output impedance is 0 under the PI control. The key points of multilayer control for parallel inverters proposed are given in follow:

(1) The first layer is an improved PQ droop method by introducing power proportional terms into a conventional droop scheme. Calculating the local active and reactive power of the inverter (P and Q), the droop values for given frequency, phase angle and amplitude, Δf_P, $\Delta \theta_P$ and Δu, are obtained. The parallel operation is realized by adjusting the voltage reference with these droop values.

(2) In order to compensate for the frequency and amplitude deviations caused by the control in the first layer and L_{pa}, a second layer is introduced. Referencing the frequency regulation for large power system and RMS control loop of an inverter, the amplitude and frequency of shared ac power bus are sensed and compared with its own amplitude and frequency references, U_{busr} and f_{busr}, respectively. And the deviations between them are used to adjust the reference to compensate the output voltage droop on both frequency and amplitude.

(3) To limit the phase deviation among the inverters within a small margin to ensure the droop method, the first layer control, valid, the third layer, a pre-synchronization control, is employed as the third layer control. The phase angle θ_{acl} of the shared ac bus voltage is sensed and used as the phase-reference. The phase angle of the inverter, θ, is measured in real time. And the θ is adjusted directly and to follow θ_{acl} roughly but rapidly when the error between θ and θ_{acl} exceeds the limitation (for example 5^0). When the error between θ and θ_{acl} falling into a small margin accepted by the droop method (for example 3^0), the synchronization is regulated by the first layer control and the pre-synchronizing is inactive. So the third layer is also a

quasi-synchronizing.

Furthermore, the pre-synchronizing allows a soft hot-swap with little inrush current may be caused by the asynchronism among the inverter at the plug-in instant.

A. The first layer: improved droop control

The conventional droop method can be with eq. (1):

$$\begin{cases} f_{rm} = f_r - \Delta f_P = f_r - k_{Pf} * P \\ U_{refmr} = U_{refm} - \Delta u = U_{refm} - k_Q * Q \\ U_{dref} = U_{refmr} \\ U_{qref} = 0 \end{cases} \tag{1}$$

where U_{refm}, proportional to f_r in U/f mode, is the amplitude of the reference signal. f_{rm} and U_{refmr} are the frequency and amplitude of reference regulated by the droop method. k_{Pf} and k_Q are the proportional coefficients of active-power-frequency and reactive-power-amplitude droops. U_{dref} and U_{qref} are voltages in the d and q axis references frame.

The improved droop method proposed is given in eq. (2).

$$\begin{cases} f_{rm} = f_r - k_{Pf} * P \\ U_{refmr} = U_{refm} - k_Q * Q \\ \Delta \theta_P = k_{P\theta} * P \\ U_{dref} = U_{refmr} \cos(0^0 - \Delta \theta_P) \\ U_{qref} = U_{refmr} \sin(0^0 - \Delta \theta_P) \end{cases} \tag{2}$$

where $k_{P\theta}$ is the proportional coefficient of active-power-phase droop.

Take two inverters in parallel as an example to explain the operational principle. The phase angle of each inverter can be obtained from (2) as in follow

$$\text{Inverter1: } \theta_1 = \int 2\pi (f_r - \Delta f_{P1}) dt - \Delta \theta_{P1} \tag{3}$$

$$\text{Inverter2: } \theta_2 = \int 2\pi (f_r - \Delta f_{P2}) dt - \Delta \theta_{P2} \tag{4}$$

Subtracting (4) from (3), the phase angle difference is

$$\begin{aligned} \theta_1 - \theta_2 &= -\int 2\pi (\Delta f_{P1} - \Delta f_{P2}) dt - (\Delta \theta_{P1} - \Delta \theta_{P2}) \\ &= 2\pi k_{Pf} \int [0 - (P_1 - P_2)] dt + k_{P\theta} [0 - (P_1 - P_2)] \end{aligned} \tag{5}$$

Eq. (5) shows clearly that the phase error, θ_1-θ_2, will be controlled by active power error (P_1-P_2) in part. And if defining $k_{P\theta}$=0, eq. (2) will degenerate to a conventional droop control.

4

The frequency of the inverter voltage is regulated by the active power, and the phase error, θ_1-θ_2, is regulated by the active power error (P_1-P_2) with an integral regulator. Therefore during steady state the active power of two inverters can be controlled equal (P_1=P_2) and the two inverters kept in phase with each other (θ_1=θ_2). That means, the system with the improved droop method is an error-less one in steady state theoretically.

If defining k_{Pf}=0, the phase angle of the inverter is regulated by active power to realize the synchronization control. And the phase error, θ_1-θ_2, is controlled by active power error (P_1-P_2) with a proportional regulator, accompanying a steady state error. Comparing with an integral regulator, the proportional one responds faster in transient process.

Summarizing the analysis above, we concludes that the power sharing performance in both steady and dynamic state is improved with the new droop method.

In addition, if the inverters with different ratings in parallel operation, the droop coefficients and L_{pa} can be selected following eq. (6).

$$\begin{cases} k_{Pf1}\Box S_1 = k_{Pf2}\Box S_2 = \cdots = k_{Pfn}\Box S_n \\ k_{P\theta1}\Box S_1 = k_{P\theta2}\Box S_2 = \cdots = k_{P\theta n}\Box S_n \\ k_{Q1}\Box S_1 = k_{Q2}\Box S_2 = \cdots = k_{Qn}\Box S_n \\ L_{pa1}\Box S_1 = L_{pa2}\Box S_2 = \cdots = L_{pan}\Box S_n \end{cases} \tag{6}$$

where S_n is the apparent power rating of the inverter n. In this paper, only the case of S_1=S_2=…=S_n is considered to simplify the analysis.

B. The second layer: load regulation compensation

A three phase current sharing inductor, L_{pa}, is normally needed between the output of the inverter and the ac bus for the droop control [6]. Because the L_{pa} is excluded in the close loop regulation of the inverter voltage, it induces the differences between the voltages on the ac bus and the inverter terminal. And the first layer droop control hurt the load regulation at the same time. So a second layer control, a compensation for load regulation, is proposed. In each inverter, both of the frequency and amplitude of the shared ac bus are sensed and compared with its own voltage reference and the deviations between them are used to adjust the reference to compensate the output voltage droop on both voltage frequency and amplitude. The effect of the second layer control is shown in Fig. 1. Where f_{rm} and U_{refmr} are the frequency and amplitude references of the inverter without the second layer control, and f_{rmc}($=f_{rm}+f_{com}$) and U_{refmrc}($=U_{refmr}+U_{mc}$) are the ones with the control mentioned. f_{com} and U_{mc} are the redeem from both of the frequency and amplitude, respectively.

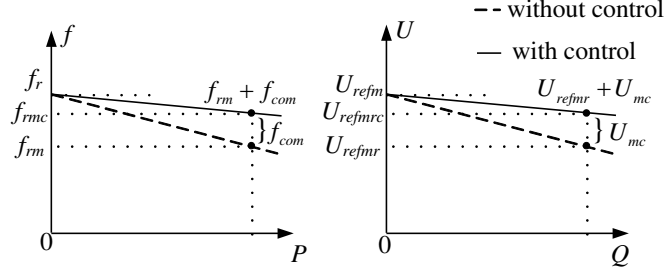The control rule is given in eq. (7).

Fig. 1 Compensation principle of the secondary control

$$
\begin{cases}
f_{rmc} = f_r - k_{Pf} * P + \underbrace{G_f * (f_{busr} - f_{buss})}_{f_{com}} \\[2mm]
U_{refmrc} = U_{refm} - k_Q * Q + \underbrace{G_u * (U_{busr} - U_{buss})}_{U_{mc}} \\[2mm]
\Delta\theta_P = k_{P\theta} * P \\[1mm]
U_{dref} = U_{refmrc} \cos(0^0 - \Delta\theta_P) \\[1mm]
U_{qref} = U_{refmrc} \sin(0^0 - \Delta\theta_P)
\end{cases}
\tag{7}
$$

where f_{busr} and U_{busr} are the frequency and amplitude references corresponding to the rated voltage of the ac bus, respectively, and f_{buss} and U_{buss} the sensed ones. G_f and G_u are the frequency and amplitude compensation coefficients, respectively.

C. The third layer: pre- and quasi- synchronization

The key point of the third layer control, as mentioned in section II, is that the inverter adjusts its own voltage reference phase angle, θ, to follow that of the shared ac power bus, θ_{acl}, directly and roughly to keep the phase error between them, $\Delta\theta_s$, within a limited margin in both steady and dynamic state.

$$
\Delta\theta_s = \theta_{acl} - \theta - 30^0
\tag{8}
$$

A positive $\Delta\theta_s$ means the inverter voltage is lagging that of the ac bus and vice versa.

The principle of the third layer control is given taking inverter j (j=1, 2, …, n) as example and using θ_{acl} as shared phase reference is shown in Fig. 2. u_{acl} and u_{acls} are the line-line voltage and its sensed signal, respectively. θ_{acl} represents the phase signal (square wave) of u_{acl}. u_{ao} is the phase voltage of the ac bus which lagging u_{acl} by 30^0 and θ_{ao} is the phase signal of u_{ao} calculated with θ_{acl} by the DSP. θ_j is the phase angle of the output voltage of inverter-j, which equals to the given phase reference before drooping. And θ_{jout} is the square wave representing the phase signal of θ_j.

Each inverter adjusts the phase of its own reference slightly every output cycle, according to the difference between θ_j and θ_{ao}, realizing the synchronization of all the inverters, as shown in Fig. 2. For example, when θ_j is leading, the adjustment value is subtracted from it. When θ_j is lagging, the adjustment value is added to it. The integral slop of θ_j is
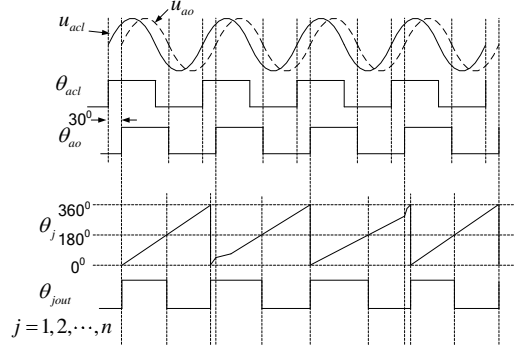
6

Fig. 2 Principle of third layer control

unchanged while decreasing or increasing the phase angle, i.e., the frequency of the inverter is fixed. Defining a function:

$$SC\_S = \begin{cases} 1 & |\Delta\theta_s| \geq SC\_\theta_{ul} \\ 1\ or\ 0 & SC\_\theta_{ll} \leq |\Delta\theta_s| < SC\_\theta_{ul} \\ 0 & |\Delta\theta_s| < SC\_\theta_{ll} \end{cases} \tag{9}$$

where SC_θ_{ul} and SC_θ_{ll} are the upper and lower limits of the errors $|\Delta\theta_s|$, respectively. SC_S is the status of the third layer active (1) or sleep (0). The logic diagram is shown in Fig. 3.
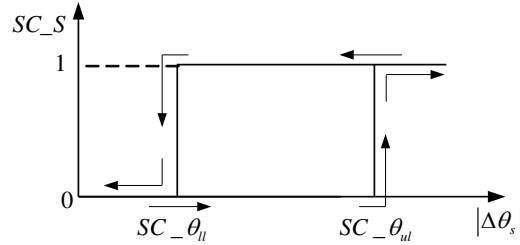

Fig. 3 Logic diagram of the third layer control

The regulation rule of the third layer control is:

$$\theta_{jsyn} = \theta_j + SC\_S \cdot k_{syn} \cdot \Delta\theta_s \tag{10}$$

where θ_{jsyn} is the regulated phase signal, k_{syn} is proportional coefficient. And $\Delta\theta_s$ can be calculated as follows according to Fig. 2.

$$\Delta\theta_s = \begin{cases} 330^\circ - \theta, & 150^\circ \leq \theta < 360^\circ \\ -\theta - 30^0, & 0^\circ \leq \theta < 150^\circ \end{cases} \tag{11}$$

Due to digital control, θ_j is accumulated in every switching period. So, the regulation rule eq. (10) can be written as:

$$\theta_{jsyn} = \left(\sum_{i=1}^{n} 360^\circ \times f_{rmc}/f_c \right) + SC\_S \cdot k_{syn} \cdot \Delta\theta_s, \quad n = f_c/f_{rmc} \tag{12}$$

7

where f_c is switching frequency. f_{rmc} is equal to f_r in pre-synchronization control while it can be calculated by eq. (7) in steady state.

With multilayer control, the phase angle θ of the inverter can be expressed as:

$$\theta = \int_0^{1/f_r} 2\pi f_{inv} * dt = \int_0^{1/f_r} 2\pi (f_r + f_{com} - k_{Pf} * P) * dt - \\ k_{P\theta} * P + SC\_S * k_{syn} * \Delta\theta_s \quad (13)$$

where f_{inv} is the output frequency of the inverter with multilayer control.

The diagram of the multilayer control proposed is shown in Fig. 4, where the multilayer control is embodied in the unit 1, 2 and 3. Unit 1 is separated into two sections which regulate the reference with the active power and reactive power, P and Q, respectively, under the improved droop method as given in eq.(2). The regulated frequency reference f_{rmc} and regulated voltage reference in dq axis, U_{dqref}, are achieved. The amplitude U_m for SVPWM is obtained by dual loop PI control. The phase θ for SVPWM is achieved after f_{rmc} getting through the phase angle calculation unit and synchronization control unit. And the drive signals by SVPWM with U_m and θ are generated to drive the switches and the parallel control is realized. As for unit 2, u_{acls} is sensed. The frequency and amplitude of common ac bus are obtained. According to eq. (7), the output of parallel system is compensated and the load regulation is improved. As for unit 3, θ_{acl} of common ac bus is achieved by regulation circuit and phase angle captured circuit. Before plugging into common ac bus, the phase angle of the inverter, θ, is
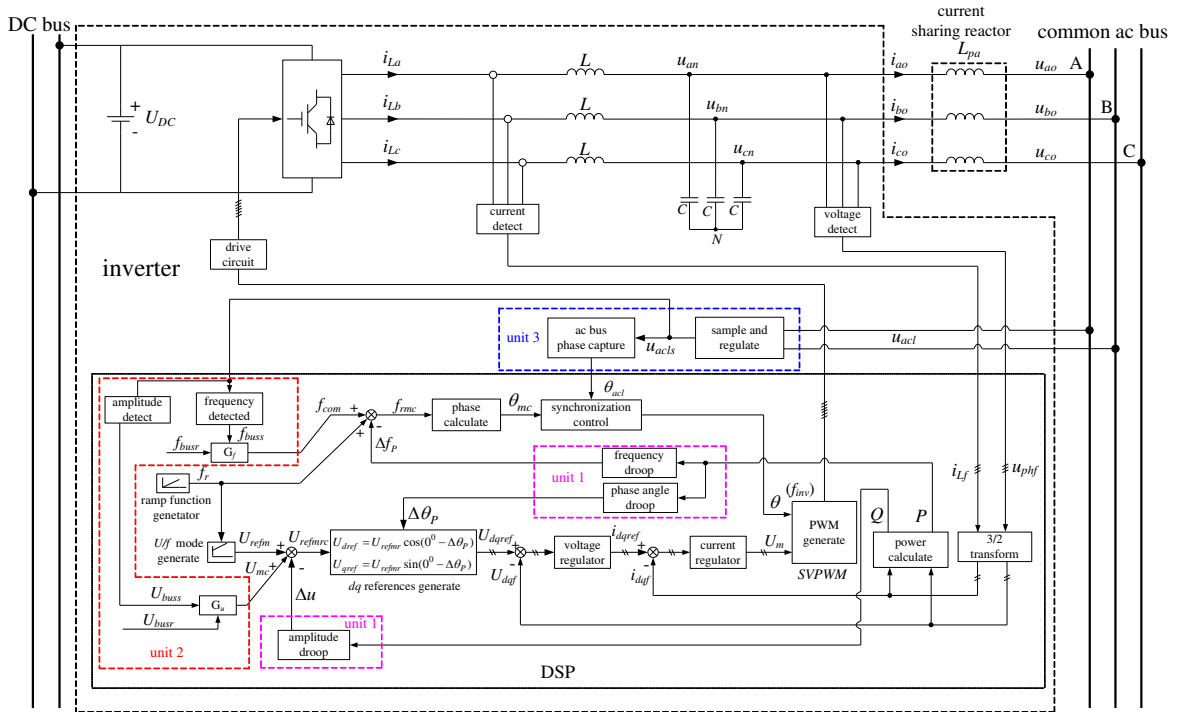

Fig. 4 The control diagram

regulated to be closed to θ_{acl} by the quasi- synchronization control in order to suppress the inrush current at hot plug-in. In steady state, θ is detected in real time. The quasi- synchronization control is employed and θ is regulated rapidly and roughly to follow θ_{acl} when the error between θ and θ_{acl} exceeds the limitation. If the error between θ and θ_{acl} within the range, the synchronization regulation is based on the first layer control and the third layer control is inactive.

In addition, the parallel system mainly feed the motor load and *U/f* control is adopted in order to avoid the current surge. And the given frequency f_r increases smoothly from 0 to its rated value (50Hz).

III. COORDINATION OF THE THREE CONTROL LAYERS

In a practical system, the amplitude error of references between each module is small, which largely depends on the parameter variations of devices. But the phase error is random and would be large without proper regulation. As a result, the control of the phase is dominant and the major purpose in all three control layers. The coordinated control for all layers should be based on coordinating synchronization control of phase angles.

In the first layer control, the phase is regulated slightly and the regulation speed is slow so that the frequency fluctuation is small, which ensures that the parallel system operates smoothly. In third layer control, the phase is regulated directly and heavily so that the regulation speed is high, which results in high frequency fluctuations. The second layer control is of the outer control loop and the time-constant is large so that the regulation speed is slow as well. The good steady-state performance of the second layer control is desired, while the dynamic performance is not so important in this layer. From above analysis, the first layer can coexist with the second layer and they complement each other. And the activation of the third layer control depends on $\Delta\theta_s$. As a result, the coordinated control relies on values of SC_θ_{ul} and SC_θ_{ll} and two aspects should be taken into consideration: (1) The third layer should not activate when the inverter operates alone, (2) The third layer control should activate in terms of the phase difference when N inverters operate in parallel with M loads.

According to the control strategy, there is no difference in phase between output voltage and the references of the inverter theoretically. However, the current sharing inductors L_{pa} are connected between the inverter and common ac bus, which causes the phase shift $\Delta\theta_{Lpa}$ between the inverter's output voltage and common ac bus voltage.

Assuming the balanced three-phase loads, the phase-*a* equivalent circuit of N inverter modules in parallel with M loads is shown in Fig. 5. $U_{ann}\angle\theta_n$ is the phase-*a* output voltage of inverter *n*. $rL_{pa}+sL_{pa}$ is the sum of output impedance and lines impedance and inductive impedance of current sharing inductors. Z is the load impedance. $U_{ao}\angle 0^0$ is the phase-*a* voltage of the common ac bus.
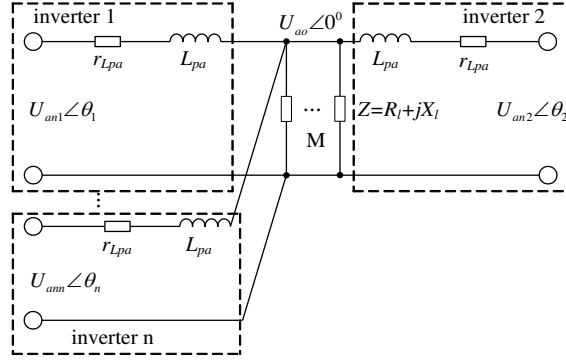
Fig. 5 The equivalent circuit of N inverter modules in parallel with M loads

(1) The inverter operating alone

From Fig. 5, assuming $rL_{pa}=0$, $\Delta\theta_{Lpa}$ can be expressed as:

$$\Delta\theta_{Lpa} = \arctan\frac{R_l\omega L_{pa}}{R_l^2 + \omega L_{pa}*X_l + X_l^2} \tag{14}$$

When operating alone, the third layer control is inactive. So,

$$SC\_\theta_{ll} > \max(\Delta\theta_{Lpa}) \tag{15}$$

And the requirement should be satisfied simultaneously:

$$SC\_\theta_{ll} < SC\_\theta_{ul} \tag{16}$$

(2) N inverter modules in parallel with M loads

Under this condition, $\Delta\theta_{Lpa}$ can be expressed as (detailed proof is given in appendix I):

$$\Delta\theta_{Lpa} = \arctan\frac{\dfrac{M}{N}R_l\omega L_{pa}}{R_l^2 + X_l^2 + \dfrac{M}{N}\omega L_{pa}*X_l} \tag{17}$$

The third layer control is inactive when the parallel system operates in steady state. So,

$$SC\_\theta_{ul} > SC\_\theta_{ll} > \max(\Delta\theta_{Lpa}) \tag{18}$$

With coordinated control, each level can complement the other well and the stability and reliability of the parallel system are enhanced.

IV. STABILITY ANALYSIS AND DESIGN CONSIDERATION

From coordinated control, it can be seen that the first layer and second layer are employed in steady state and starting third layer means the system is in unstable region. As a result, in order to study the stability and the transient response of the

system, the third layer is ignored.

The time-constant of second layer control is over one decade below from the one of first layer control. For the first layer control, the effect of the second layer regulation is a very slow disturbance. And the compensation values (f_{com}, U_{mc}) are invariable when the first layer control is active. As a result, the second layer loop can be opened when studying the stability of the first layer control.

Similarly, the dynamic response of first layer control is very faster than that of second layer control. As a result, the first layer loop can be simplified to be a proportion loop when analyzing the stability of the second layer.

According to above analysis, the first layer is analyzed with the second layer loop opened. A small-signal analysis is presented.
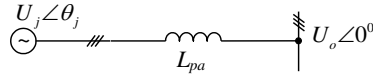

Fig. 6 Equivalent circuit of inverter j connected to common ac bus

Fig 6 shows the equivalent circuit of inverter j connected to the common ac bus which is shown in detail in Fig. 5. In Fig. 6, $U_j \angle \theta_j$ is the three-phase output voltage of inverter j and $U_o \angle 0^0$ is the three-phase voltage of common ac bus. $U_j = U_{anj} = U_{bnj} = U_{cnj}$, $U_o = U_{ao} = U_{bo} = U_{co}$.

Assuming the balanced three-phase loads, the active and reactive powers of inverter j calculated with output voltage and inductor currents can be expressed as:

$$\begin{cases} P_j = 3\dfrac{U_j U_o}{X_{Lpa}} \sin \theta_j \\ Q_j = 3[\dfrac{U_j U_o \cos \theta_j - U_o^2}{X_{Lpa}} - U_j^2 X_C] \end{cases} \tag{19}$$

where $X_{Lpa} = \omega L_{pa}$, $X_C = \omega C$.

And from (2), it can be achieved as follows

$$\begin{cases} \theta_j = \theta_j^* - \displaystyle\int_{-\infty}^{t} k_{Pf} P_j d\tau - k_{P\theta} P_j \\ U_j = U_j^* - k_Q Q_j \end{cases} \tag{20}$$

where U_j^* and θ_j^* are the output voltage phase and amplitude at no load.

As mentioned above, the phase error is the main reason for causing the circulating currents among the inverters. Consequently, a small-signal analysis is presented to obtain the dynamics of θ_j. First, the small-signal dynamics of the

11

active and reactive power are obtained by linearizing (19) and modeling the low-pass filters with a first-order description

$$
\begin{cases}
p_j = \dfrac{3\omega_{cut}}{s+\omega_{cut}} \dfrac{U_o}{X_{Lpa}} [\sin\theta_j \hat{u}_j + U_j \cos\theta_j \hat{\theta}_j] \\[3mm]
q_j = \dfrac{3\omega_{cut}}{s+\omega_{cut}} \{ \dfrac{U_o}{X_{Lpa}} [\cos\theta_j \hat{u}_j - U_j \sin\theta_j \hat{\theta}_j] - 2U_j X_C \hat{u}_j \}
\end{cases}
\tag{21}
$$

where ^ denotes perturbed values, capital letters mean equilibrium point values, and ω_{cut} is the cut-off angular frequency of the low-pass filters, which should be fixed over one decade below from frequency mains.

Second, by perturbing (20) using (21), the small variations of θ_j and U_j can be obtained:

$$
\hat{\theta}_j = -(\dfrac{k_{Pf}}{s} + k_{P\theta}) \dfrac{3\omega_{cut}}{s+\omega_{cut}} \dfrac{U_o}{X_{Lpa}} \times
\tag{22}
$$
$$
[\sin\theta_j \lfloor \hat{u}_j + U_j \cos\theta_j \lfloor \hat{\theta}_j]
$$

$$
\hat{u}_j = -k_Q \dfrac{3\omega_{cut}}{s+\omega_{cut}} \times
\tag{23}
$$
$$
\{ \dfrac{U_o}{X_{Lpa}} [\cos\theta_j \lfloor \hat{u}_j - U_j \sin\theta_j \hat{\theta}_j] - 2U_j X_C \hat{u}_j \}
$$

Finally, substituting (23) into (22), the small signal dynamics of the closed-loop system can be obtained:

$$
s^3 \hat{\theta}_j + As^2 \hat{\theta}_j + Bs \hat{\theta}_j + C \hat{\theta}_j = 0
\tag{24}
$$

where

$$
A = \dfrac{\omega_{cut}}{X_{Lpa}} [2X_{Lpa} + 3k_Q(U_o \cos\theta_j - 2X_{Lpa}X_C U_j) + 3k_{P\theta}U_o U_j \cos\theta_j]
$$

$$
B = \dfrac{\omega_{cut}}{X_{Lpa}} [\omega_{cut}X_{Lpa} + 3k_{Pf}U_o U_j \cos\theta_j + 3k_{P\theta}\omega_{cut}U_o U_j \cos\theta_j + \dfrac{9k_{P\theta}k_Q\omega_{cut}U_o U_j(U_o - 2X_{Lpa}X_C U_j \cos\theta_j)}{X_{Lpa}} +
$$
$$
3k_Q\omega_{cut}(U_o \cos\theta_j - 2X_{Lpa}X_C U_j)]
$$

$$
C = \dfrac{\omega_{cut}}{X_{Lpa}} [3k_{Pf}\omega_{cut}U_o U_j \cos\theta_j + \dfrac{9k_{Pf}k_Q\omega_{cut}U_o U_j(U_o - 2X_{Lpa}X_C U_j \cos\theta_j)}{X_{Lpa}}]
$$

Using (24), the stability of the first layer close-loop system can be studied, and a desired transient response can be selected following a linear third-order dynamics.

Fig 7(a) and (b) show the root locus plots using the parameters listed in Table I with considering a variation of the coefficients k_{Pf} and $k_{P\theta}$. Notice that the system has three roots, λ_1, λ_2 and λ_3. The arrows indicate the evolution of the corresponding pole when the coefficient increases. In Fig. 7(a), with the increasing of $k_{P\theta}$, the conjugated poles tend to go

far away from the imaginary axis splitting as two real poles and the single real pole becomes the complex pole. Fig 7(b) shows that when k_{Pf} increases, the complex poles become dominant, resulting in a near second order behavior. And the dynamic response of the system turns to be faster. Since both cases the poles are located in the left half s-plane, the system is stable.

Table I

PARAMETERS OF THE FIRST LAYER CONTROL

Item	Symbol	Nominal Value	Unit
Current sharing inductor	L_{pa}	0.8	mH
Filter capacitor	C	50	μF
Nominal frequency	ω	$2\pi \cdot 50$	rad/s
Nominal voltage	U	220	V
Power filters cut-off frequency	ω_{cut}	10	rad/s
P-f droop coefficient	k_{Pf}	1×10^{-5}	rad/(W·s)
P-θ droop coefficient	$k_{P\theta}$	2×10^{-8}	rad/W
Q-U droop coefficient	k_Q	2.15×10^{-4}	V/Var
Initial phase difference	θ_0	0.05	rad

(a)   (b)
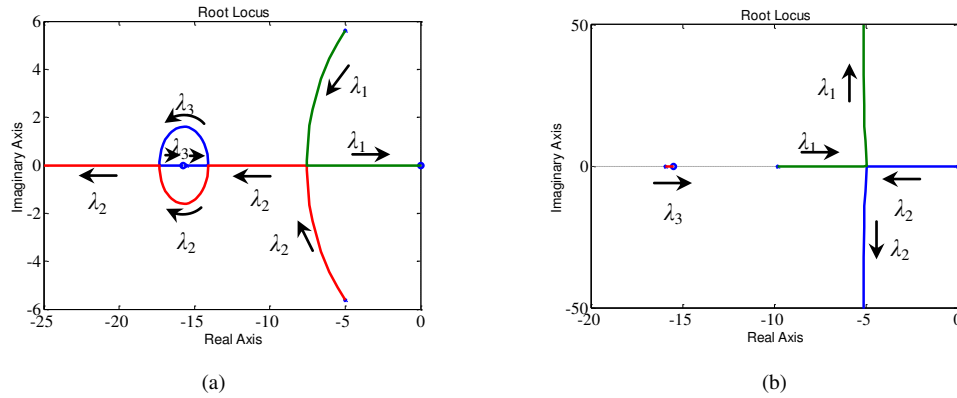
Fig. 7 Root locus diagrams for (a) $k_{P\theta}$, k_{Pf}=1·10-5, k_Q=2.15·10-4 and (b) k_{Pf}, $k_{P\theta}$=2.·10-8, k_Q=2.15·10-4.

Thus, the stability of first layer control is proved and the coefficients can be chosen in practical design to obtain the desired transient response performance using the analysis method above.

On analyzing the stability of second layer control, the first layer is simplified to be a proportion loop k_{FL}. And in the practice system, the proportion controllers are adopted as the compensators, G_f and G_u, in eq. (7). The frequency control diagram of second layer is shown in Fig. 8 and the loop is a conventional proportional feedback loop. The stability of second layer control is easy to prove and the detail analysis isn't given here.

13

f_r

f_{busr} + → ◯ → G_f → + ◯ + → k_{FL} → f_{bus}

− f_{buss} *P* controller

Filter with large time-constant
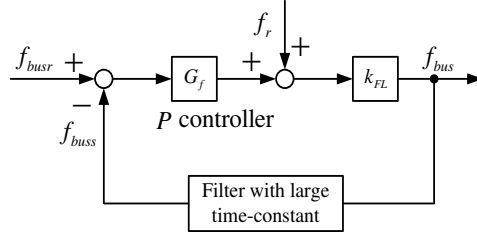
V. EXPERIMENTAL RESULTS

A prototype system with two DSP (TMS320F2812) controlled inverters in parallel is built. The configuration and control is shown in Fig. 4. The DC bus voltage is 600V and rated output voltage is 380V/50Hz. The designed capacity is 35kVA and switch frequency is 6kHz. The value of L is 0.6mH and C is 50μF while L_{pa} is 0.8mH. The resistive and non-linear loads are used in the experiment.

In Fig. 9, Fig. 10 and Fig. 11, u_{an1} u_{an2} are the phase a voltages of inverter 1 and inverter 2, and i_{La1} and i_{La2} are the phase a inductor currents. i_{ao1} and i_{ao2} are the phase a output currents of inverter 1 and inverter 2 while i_{ao} is the phase a load current which is equal to $i_{ao1}+i_{ao2}$. u_{ab} is the line-line voltage of common ac bus. θ_{1out} and θ_{2out} are the representation signals of phase angle of inverter 1 and inverter 2 shown in Fig. 2.

The result of transient performance under hot swapping is shown in Fig. 9. As shown in Fig. 9, the parallel system gets into steady state after the transient regulation with small inrush current and voltage fluctuation. And the phase error at hot-plug is small with introduced the quasi-synchronization control. The result shows a good performance of parallel control during hot plug-in.

The results of parallel operation with stepping resistive load are shown in Fig. 10. Fig. 10 (a) shows load step up from 0 to 16kW while Fig. 10 (b) shows the load step down from 16kW to no load. The results indicate that the proposed parallel control has good dynamic performance.

The steady-state parallel operation results are given in Fig. 11. Fig.11 (a) shows the steady state waveforms at 37kW resistive load. Fig. 11 (b) shows the phase error between two inverters under the condition of Fig. 11(a). Fig. 11(c) shows the result when the system supplying a non-linear load. The results shows that the proposed parallel control has good performance at steady state even when supplying nonlinear load and the phase error is smaller than 0.36^0 ($\pm20\mu$s).

Fig. 12 shows the result of second layer control with 37kW resistive load. With the compensation, the deviation of system output voltage is decreased to 2.5V RMS compared to 3.5V RMS without second layer control.

VI. CONCLUSION

A multilayer control scheme for inverters in parallel operation without interconnection is proposed and analysis and implementation are given. The first layer control is based on the improved droop method by introducing power proportional terms into a conventional droop scheme. With the help of the first layer control, the dynamic and steady state performances are enhanced. The second layer control compensates the output voltage deviations, which are caused by droop method and L_{pa}, through sensing the frequency and amplitude of common ac bus. With the third layer control, the phase of common ac bus is sensed and the phase of inverter is regulated when the phase error between inverter and common ac bus is out of range and thus losing synchronism is avoided. Moreover, the pre-synchronization control regulates the phase of inverters before hot-plug into the common ac bus and as a result, the inrush currents are suppressed and the stability of the system is enhanced. Experimental results are given to validate the proposed control approach, showing good power sharing when supplying linear and nonlinear loads.
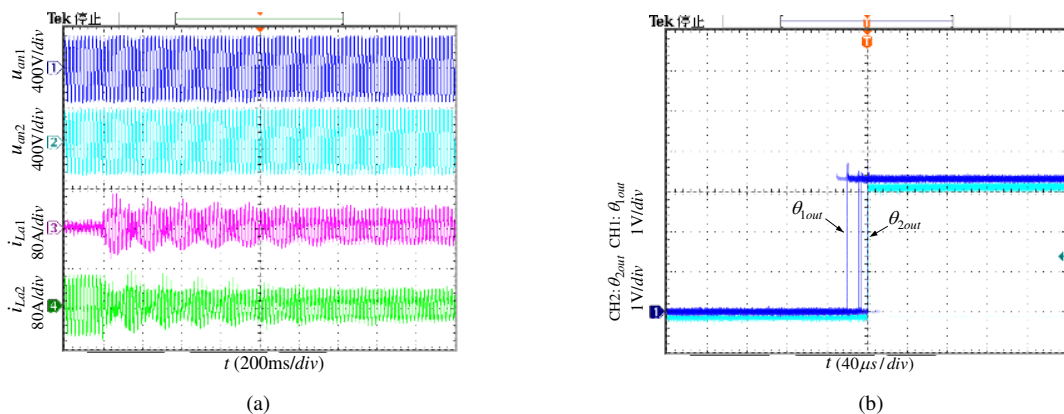

Fig. 9 Experimental result with hot-plug in: (a) Voltage and inductor current, (b) Phase error at hot-plug in.
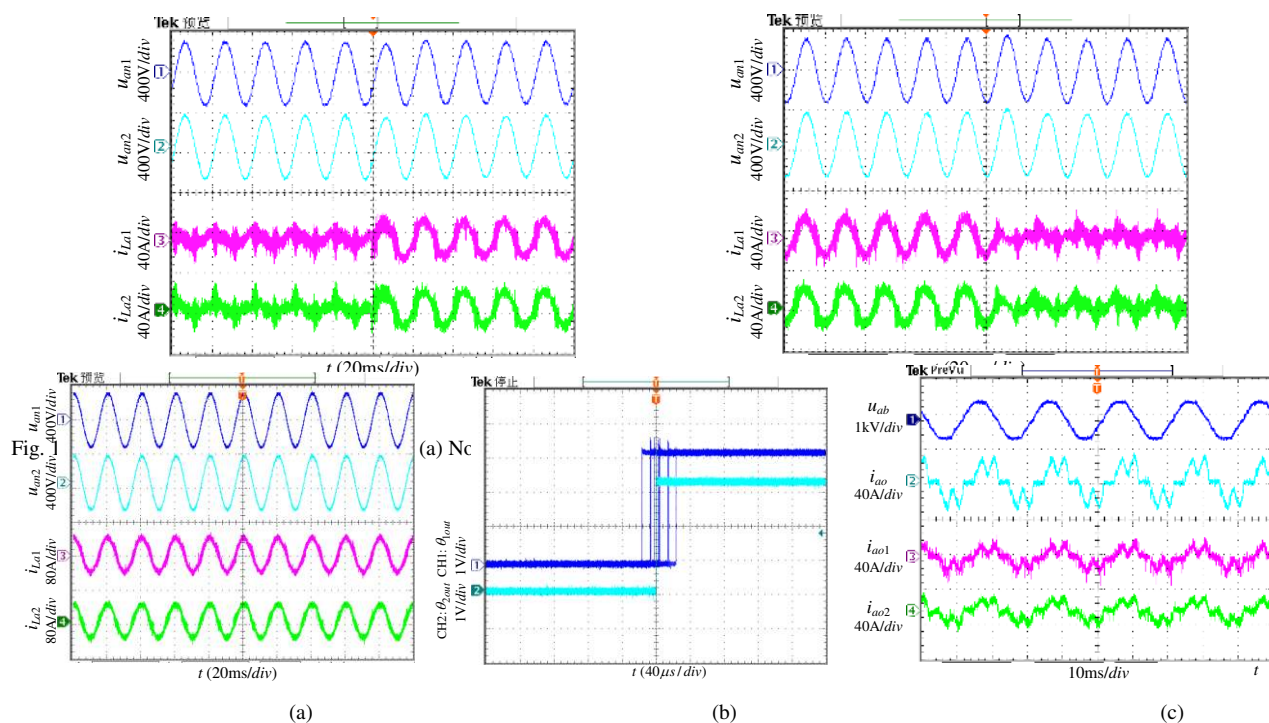

Fig. 11 Experimental result in steady state: (a) 37kW, (b) Phase error between two inverters, (c) Supplying non-linear load.
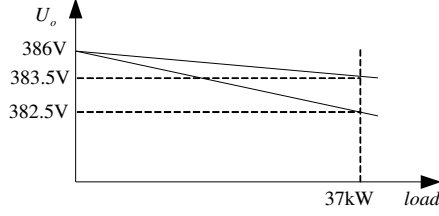
Fig. 12 Voltage compensation of Second layer control.

VII. APPENDIX I

Assuming r_{Lpa} is equal to 0, it can be achieved as follows from Fig. 5:

$$\frac{U_{an1}\angle\theta_1 - U_{ao}\angle 0}{j\omega L_{pa}} + \cdots + \frac{U_{ann}\angle\theta_n - U_{ao}\angle 0}{j\omega L_{pa}} = \frac{MU_{ao}\angle 0}{Z} \quad (A1)$$

Namely

$$\frac{U_{an1}\angle\theta_1 + \cdots + U_{ann}\angle\theta_n}{j\omega L_{pa}} = \frac{MU_{ao}\angle 0}{Z} + \frac{NU_{ao}\angle 0}{j\omega L_{pa}} \quad (A2)$$

The PI controller in dq rotation frame is applied to control the inverter so that the model of the inverter can be viewed as a DC system. It's easy to control voltage amplitude of each inverter equal to the other. So, assuming that amplitudes of voltages of all parallel inverters are equal ($U_{an1}=U_{an2}=\ldots=U_{ann}$) in steady state. With the first layer control, all the parallel inverters keep in phase with each other ($\theta_1=\theta_2=\ldots=\theta_n$). According to above, (A2) is approximately equivalent to

$$\frac{NU_{an1}\angle\theta_1}{j\omega L_{pa}} = \frac{MU_{ao}\angle 0}{Z} + \frac{NU_{ao}\angle 0}{j\omega L_{pa}} \quad (A3)$$

So

$$U_{an1}\angle\theta_1 = U_{ao}\angle 0(1 + \frac{j\omega L_{pa}M}{NZ}) \quad (A4)$$

With substituting R_l+jX_l for Z, equation (A4) can be expressed as:

$$U_{an1}\angle\theta_1 = U_{ao}\angle 0 \frac{NR_l + j(NX_l + \omega L_{pa}M)}{NR_l + jNX_l} \quad (A5)$$

From equation (A5), it can be achieved:

$$\Delta\theta_{Lpa} = |\theta_1| = \arctan\frac{\dfrac{M}{N}R_l\omega L_{pa}}{R_l^2 + X_l^2 + \dfrac{M}{N}\omega L_{pa}*X_l} \quad (A6)$$

The maximal value of Equation (A6) is related to the number of parallel inverters with loads and the types of loads.

16

VIII. References

[1] Z. He, Y. Xing, "Distributed control for UPS modules in parallel operation with RMS voltage regulation," IEEE Trans. Ind. Electron., vol. 55, no. 8, pp. 2860-2869, 2008.

[2] Y. Xing, L. Huang, and Y. Yan, "Redundant parallel control for current regulated inverters with instantaneous current sharing," in Proc. IEEE Power Electron. Spec. Conf., 2003, pp. 1438-1442.

[3] J. M. Guerrero, J. Matas J, L. G. de Vicuña, et al., "Decentralized control for parallel operation of distributed generation inverters using resistive output impedance," IEEE Trans. Ind. Electron., vol. 54, no. 2, pp. 994-1004, 2007.

[4] J. M. Guerrero, L. G. de Vicuña, J. Matas, M. Castilla, and J. Miret, "Wireless-control strategy for parallel operation of distributed-generation inverters." IEEE Trans. Ind. Electron., vol. 53, no. 5, pp. 1461-1470, Oct. 2006.

[5] K. de Brabandere, B. Bolsens, J. Van den Keybus, et al., "A voltage and frequency droop control method for parallel inverters," IEEE Trans. Power Electron., vol. 22, no. 4, pp. 1107-1115, 2007.

[6] J. M. Guerrero, L. G. de Vicuña, J. Matas, M. Castilla, and J. Miret, "Output impedance design of parallel-connected UPS inverters with wire-less load-sharing control," IEEE Trans. Ind. Electron., vol. 52, no. 4, pp. 1126-1135, Aug. 2005.

[7] J. M. Guerrero, L. G. de Vicuña, J. Matas, et al., "A wireless controller to enhance dynamic performance of parallel inverters in distributed generation systems," IEEE Trans. Power Electron.，vol. 19, no. 5, pp. 1205-1213, 2004.

[8] W. Yao, M. Chen, M. Gao, Z. Qian, "A wireless load sharing controller to improve the performance of parallel-connected inverters," IEEE APEC, 2008, pp. 1628-1631.

[9] D. De and V. Ramanarayanan, "Decentralized parallel operation of inverters sharing unbalanced and nonlinear loads," IEEE Trans. Power Electron., vol. 25, no. 12, pp. 3015-3025, 2010.

[10] D. De and V. Ramanarayanan, "A proportional + multiresonant controller for three-phase four-wire high-frequency link inverter," IEEE Trans. Power Electron., vol. 25, no. 4, pp. 899-906, 2010.

[11] M. Dai, M. N. Marwali, J.-W. Jung and A. Keyhani, "Power flow control of a single distributed generation unit," IEEE Trans. Power Electron., vol. 23, no. 1, pp. 343-352, 2008.

[12] R. Majumder, G. Ledwich, A. Ghosh, et al, "Droop control of converter -interfaced microsources in rural distributed generation," IEEE Trans. Power Del., vol. 25, no. 4, pp. 2768-2778, 2010.

[13] N. Pogaku, M. Prodanović and T. C. Gree, "Modeling, analysis and testing of autonomous operation of an inverter-based microgrid," IEEE Trans. Power Electron., vol. 22, no. 2, pp. 613-625, 2007.

[14] C. K. Sao and P. W. Lehn, "Autonomous load sharing of voltage source converters," IEEE Trans. Power Del., vol. 20, no. 2, pp. 1009-1016, 2005.

[15] Y. Li, D. M. Vilathgamuwa and P. C. Loh, "Design, analysis, and real-time testing of a controller for multibus microgrid system," IEEE Trans. Power Electron., vol. 19, no. 5, pp. 1195-1204, 2004.

[16] W. Yao, M. Chen, J. Matas, J. M. Guerrero, et al, "Design and analysis of the droop control method for parallel inverters considering the impact of the complex impedance on the power sharing," IEEE Trans. Ind. Electron., vol. 58, no. 2, pp. 576-588, 2011.

[17] T. B. Lazzarin, G. A. T. Bauer and I.Barbi, "A control strategy by instantaneous average values for parallel operation of single phase voltage source inverters based in the inductor current feedback," in Proc. IEEE ECCE, 2009, pp. 495-502.

[18] J. C. Vasquez, J. M. Guerrero, M. Liserre, A. Mastromauro, "Voltage support provided by a droop-controlled multifunctional inverter," IEEE Trans. Ind. Electron., vol. 56, no. 11, pp. 4510-4519, 2009.

[19] X. Zhang, H. Zhang, X. Ma and J. M. Guerrero, "Sharing of active power supply and reactive power compensation for parallel inverters," in Proc. IEEE APEC, 2009, pp. 353-357.

[20] Z. Ren, M. Gao, Q. Mo and K. Liu, et al, "Power calculation method used in wireless parallel inverters under nonlinear load conditions," in Proc. IEEE APEC, 2010, pp. 1674-1677.

[21] C. -T. Lee, C. -C. Chu and P. -T. Cheng, "A new droop control method for the autonomous operation of distributed energy resource interface converters," in Proc. IEEE ECCE, 2010, pp. 702-709.

[22] J. C. Vasquez, J. M. Guerrero, A. Luna, P. Rodriguez, et al, "Adaptive droop control applied to voltage-source inverters operating in Grid-connected and islanded modes," IEEE Trans. Ind. Electron., vol. 56, no. 10, pp. 4088-4096, 2009.

[23] E. Barklund, N. Pogaku, M. Prodanovic, C. Hernandez-Aramburo, et al, "Energy management in autonomous microgrid using stability-constrained droop control of inverters," IEEE Trans. Power Electron., vol. 23, no. 5, pp. 2346-2352, 2008.

[24] A. Hasanzadeh, O. C. Onar, H. Mokhtari, and A. Khaligh, "A proportional-resonant controller-based wireless control strategy with a reduced number of sensor for parallel-operated UPSs," IEEE Trans. Power Del., vol. 25, no. 1, pp. 468-478, 2010.

[25] X. Lin, S. Duan, Y. Kang and J. Chen, "A new decoupling control scheme for the parallel operation of UPS," Journal of Electrical Engineering, vol. 54, no. 1-2, pp. 46-51, 2003.

[26] M. C. Chandorkar, D. M. Divan, Y. Hu, and B. Banerjee, "Novel architectures and control for distributed UPS systems," IEEE APEC, 1994, pp. 683-689.

[27] J. M. Guerrero, J. C. Vásquez, J. Matas, et al, "Control strategy for flexible Microgrid based on parallel line-interactive UPS systems," IEEE Trans. Ind. Electron., vol. 56, no. 3, pp. 726-736, 2009.

[28] Y. W. Li and C.-N. Kao, "An accurate power control strategy for power-electronics-interfaced distributed generation units operating in a low-voltage multibus microgrid," IEEE Trans. Power Electron., vol. 24, no. 12, pp. 2977-2988, 2009.

[29] P. Kundur. Power System Stability and Control. McGraw-Hill Professional, 1994.

[30] J. M. Guerrero, J. C. Vásquez, J. Matas, L. G. de Vicuña, et al, "Hierarchical control of droop-controlled AC and DC Microgrids-A general approach toward standardization," IEEE Trans. Ind. Electron., vol. 58, no. 1, pp. 158-172, 2011.

[31] M. Hua, H. Hu, Y. Xing, Z. He, "Distributed control for AC-motor-drive-inverters in parallel operation," IEEE Trans. Ind. Electron., vol. PP, no. 99, pp. to appear, 2011.